# ESTIMATING REPRODUCIBLE FUNCTIONAL NETWORKS ASSOCIATED WITH TASK DYNAMICS USING UNSUPERVISED LSTMS

*Nicha C. Dvornek*\*\*, *Pamela Ventola*†, and *James S. Duncan*\*\*‡

\*Radiology & Biomedical Imaging and <sup>†</sup>Child Study Center, Yale School of Medicine, New Haven, CT \*Biomedical Engineering and <sup>‡</sup>Electrical Engineering, Yale University, New Haven, CT

# **ABSTRACT**

We propose a method for estimating more reproducible functional networks that are more strongly associated with dynamic task activity by using recurrent neural networks with long short term memory (LSTMs). The LSTM model is trained in an unsupervised manner to learn to generate the functional magnetic resonance imaging (fMRI) time-series data in regions of interest. The learned functional networks can then be used for further analysis, e.g., correlation analysis to determine functional networks that are strongly associated with an fMRI task paradigm. We test our approach and compare to other methods for decomposing functional networks from fMRI activity on 2 related but separate datasets that employ a biological motion perception task. We demonstrate that the functional networks learned by the LSTM model are more strongly associated with the task activity and dynamics compared to other approaches. Furthermore, the patterns of network association are more closely replicated across subjects within the same dataset as well as across datasets. More reproducible functional networks are essential for better characterizing the neural correlates of a target task.

*Index Terms*— Functional Networks, Task fMRI, Recurrent Neural Networks, Unsupervised Learning

## 1. INTRODUCTION

The canonical approach to task-based functional magnetic resonance image (fMRI) analysis has been mass univariate analysis at the voxel level [1]. While this allows for potentially high specificity in locating brain regions that activate with task, the noisy fMRI data lends to many false positives and the relationship between voxels in different regions is ignored. Summarizing the voxel data by regions of interest (ROIs) helps to alleviate the noisy signal problem, although regressing task against individual ROIs again ignores the potential relationships between distinct brain regions.

A multivariate approach that analyzes functional brain networks allows for a higher systems-level view of neurocognitive functions that are associated with a given task. In

This work was supported by NIH grants R01MH100028 and R01NS035193.

addition, considering several brain regions in a network may better characterize the task-associated activity and allow for a more robust representation of task-related brain changes.

The functional brain activity can be decomposed into separate networks using standard statistical tools such as principal component analysis (PCA) and independent component analysis (ICA). However, a challenge in determining functional networks, and more generally in fMRI analysis, is the question of reproducibility. The number of subjects in a task fMRI study is often smaller, making reproducibility of results challenging. While traditional methods for finding functional networks are based on analytical approaches that fit an entire dataset, predictive methods that look to generalize well to new data may improve the reproducibility of functional networks.

In this paper, we propose to use recurrent neural networks with long short term memory (LSTMs) [2] to estimate more reproducible functional networks which are strongly associated with task dynamics. Recently, LSTMs have been applied to fMRI data, e.g., to model the fMRI activity given a stimulus input [3] and for classification tasks based on fMRI [4]. We focus on using the LSTM's strength in signal generation, as demonstrated in applications such as text generation [5]. We describe how the functional networks can be estimated with unsupervised training of the LSTM model and then used for followup task-based analysis. We show improved association of functional networks with task dynamics and more reproducible results within and across 2 task fMRI datasets.

## 2. METHODS

## 2.1. LSTM for fMRI Signal Prediction

The use of an LSTM-based network for fMRI data generation was recently proposed by Dvornek et al. [4] for use as an auxiliary task to enhance learning of a discriminative task. We adopt the basic framework but focus solely on the unsupervised learning task of predicting the fMRI time-series data for N ROIs at time  $x_{T+1} \in R^N$  given the time-series data from the previous T time points  $\{x_1, \ldots x_T\}$ . The ROI timeseries data for T time points are directly input into an LSTM layer with K units. The output of the LSTM layer, i.e., the hidden state  $h_T \in R^K$ , is then fed to a fully connected layer

<sup>© 2020</sup> IEEE. Personal use of this material is permitted. Permission from IEEE must be obtained for all other uses, in any current or future media, including reprinting/republishing this material for advertising or promotional purposes, creating new collective works, for resale or redistribution to servers or lists, or reuse of any copyrighted component of this work in other works.

with N nodes, representing the N ROI signals at time T+1. Note that while the network is trained in a supervised manner, this approach is truly unsupervised, as no labels or additional information about the data is required.

The functional networks will be represented by the K units of the LSTM. The network tries to learn the interaction between the N individual ROIs and the K functional networks by generating the ROI time-series data from the decomposed functional networks,

$$\widehat{x_{T+1}} = W_f h_T + b_f,$$

where  $\widehat{x_{T+1}}$  is the predicted ROI signal at time T+1,  $W_f$  is a matrix of weights, and  $b_f$  is a vector of biases. The membership to a functional network k is defined by the weights in column k of  $W_f$ . Different from [4], we include both L1 regularization (controlled by a hyperparameter l) and a nonnegative constraint on the weights  $W_f$ . This encourages functional networks to have sparse ROI membership and to work in a cooperative manner to produce the ROI signals.

## 2.2. Functional Networks Associated with Task Dynamics

To determine functional networks that are associated with a given task performed during the fMRI scan, we perform a group-wise analysis. While any method can be applied (for example, a general linear model), here we measure the correlation between the expected fMRI signal based on the task design and the activity of the functional networks. First, the task stimulus design is convolved with a canonical hemodynamic response function. We also compute the temporal derivative of the expected fMRI response. While all subjects in a dataset perform the same task, the timing of each individual run contains very small variations. Thus, we average the expected fMRI responses and their derivatives across all subjects to obtain a mean ideal signal and its derivative, which we refer to in the following as the task design signals.

The activity of the functional networks is represented by the output of the LSTM layer,  $h_t$ , i.e.,  $h_t(k)$  represents the activity of functional network k at time t. For each subject, we extract the output of the LSTM for every time point  $t \geq T$  (since the first T time points are required for fMRI signal prediction). We then average the LSTM outputs across all subjects to obtain the mean activity of each functional network.

Finally, we compute the correlation between the mean expected fMRI signal (from time T to the end of the scan) and the mean activity of each functional network, and the correlation between the mean temporal derivative of the expected fMRI signal and the mean activity of each functional network. A functional network with high correlation with the mean expected fMRI signal is associated with the task activity itself. A functional network with high correlation with the mean derivative of the expected fMRI signal is associated with  $dynamic\ changes$  in the task. For example, in a task paradigm with block design, the functional network would be associated with the switching between 2 conditions.

#### 3. EXPERIMENTS

## 3.1. Data and Preprocessing

Data were acquired for 2 separate datasets (originally for different studies) using the same biological motion perception paradigm [6], protocol, and scanner. Each subject viewed a series of alternating blocks of point-light displays of biological motion and scrambled biological motion (~24 s/block, 6 of each condition). Dataset 1 included 82 children with autism (age =  $10.79 \pm 3.23$  years, IQ =  $83.88 \pm 43.92$ ) and 48 typical controls (age =  $9.31 \pm 3.90$  years, IQ =  $86.38 \pm 34.20$ ) matched for age and IQ. Dataset 2 included 21 children with autism (age =  $6.05 \pm 1.24$  years, IQ =  $102.00 \pm 17.87$ ) and 19 typical controls (age =  $6.42 \pm 1.29$  years, IQ =  $111.47 \pm 14.45$ ), again matched for age and IQ. Each subject underwent a BOLD fMRI scan (TR = 2000 ms, TE = 25 ms, flip angle =  $60\circ$ , voxel size =  $3.44 \times 3.44 \times 4 \text{mm}^3$ ) acquired on a Siemens MAGNETOM Trio TIM 3T scanner.

Images were preprocessed in FSL [7], including motion correction, interleaved slice timing correction, brain extraction, 4D mean intensity normalization, spatial smoothing (5 mm FWHM), data denoising via ICA-AROMA [8], nuisance regression using white matter and cerebrospinal fluid, and high-pass temporal filtering (100 s). Functional MRI were registered to the standard MNI brain and parcellated into 90 cerebral brain regions using the AAL atlas [9]. The mean time-series (146 and 156 time points for Dataset 1 and 2, respectively) was extracted from each ROI and standardized (subtracted the mean and divided by the standard deviation).

To effectively train the LSTM models, we augmented the data for each subject by extracting all possible windows of data with length  $T=30~(60~{\rm s}$  of scan time). Thus, the LSTM network receives inputs of size  $30\times 90$ . Dataset 1 was augmented from 130 to a total of 15080 samples, while Dataset 2 was augmented from 40 to a total of 5040 samples.

## 3.2. Experimental Methods

The proposed LSTM models for generating fMRI time-series data were trained separately for each dataset. We implemented the models in Keras using the mean squared error loss function, l=0.0001 for the L1 weight regularization of  $W_f$  for the fully connected layer, the AMSGrad variant [10] of the Adam optimizer (learning rate = 0.001), a batch size of 32, and 20 epochs of training. The best epoch was chosen based on the minimum loss of a monitored validation set.

We compared the proposed LSTM method to 3 other approaches: 1) Using the original ROIs. We considered each "network" to contain only 1 ROI, to investigate the potential advantages of truly functional network approaches. 2) Using principal component analysis (PCA). The ROI timeseries data for all subjects was concatenated across time and PCA was performed. The functional networks were then defined by the principal components, and the activity of each

network was given by the score from projecting the data onto the principal components. 3) Using independent component analysis (ICA). Again, the data for all subjects was concatenated across time. Group ICA [11] using the fastICA package for MATLAB [12] with default parameters was performed. The functional networks were then defined by the independent components, and the activity of each network was given by the mixing matrix. For each of the network analysis approaches, we tried 2 values for the number of functional networks K (i.e., number of LSTM units or number of principal/independent components): 25 or 50.

For model evaluation, we used 10-fold cross-validation of each dataset, with 10% for testing and 90% for training. For the LSTM models, 10% of the training data was withheld as validation data. Partitions of the dataset were performed in a subjectwise manner, such that all samples from the same subject are kept in the same partition. We computed the correlations between estimated functional networks and the design signals (task activity and task dynamics for the 2 task stimuli), resulting in 4 correlation vectors with length K:  $c_{BA}$  (biological motion activity),  $c_{BD}$  (biological motion dynamics),  $c_{SA}$  (scrambled motion activity), and  $c_{SD}$  (scrambled motion dynamics). The correlations were computed for data in the training set, as well as separately the test set.

We assessed the overall ability of the estimated functional networks to capture task-relevant activity by the maximum and minimum correlations for each design signal. Furthermore, we assessed the reliability and reproducibility of the estimated functional networks in 2 ways. First, to assess within dataset robustness, for each design signal we measured the correlation of the corresponding computed measures between the training and test sets (e.g., correlation between  $c_{BA}$  computed from training and test data). We expect that for a reproducible functional network, the same correlation between that network's activity and the task design signals should be observed in the training and test sets. Second, to assess robustness across datasets, we took the functional networks localized in Dataset 1 (2), extracted the corresponding activity for these networks in Dataset 2 (1), and measured the maximum/minimum correlations in the test sets. Reliable functional networks that capture task-relevant activity should produce large correlations with the task design signal in the independent dataset. Paired two-tailed t-tests were used to compare the corresponding results from different methods across cross-validation folds, with significance level  $\alpha = 0.05$ .

## 3.3. Results and Discussion

Results for Dataset 1 are shown in Figs. 1 and 2, and results for Dataset 2 are shown in Figs. 3 and 4. Cyan markers denote statistically significantly different results compared to our LSTM method.

Similar trends can be observed across datasets and different numbers of functional networks to be estimated *K*. Cor-

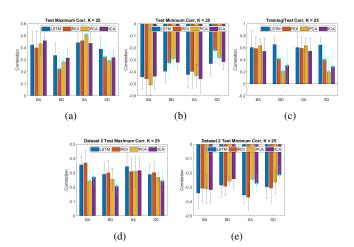


**Fig. 1**: Results for Dataset 1, with K=25 networks. (a) Maximum and (b) minimum correlation between functional network activity and task design signals. (c) Correlation between patterns of activity associated with task design signals from the training and test set. (d) Maximum and (e) minimum correlation between functional network activity in Dataset 2 using networks estimated by Dataset 1 and task design signals. BA = biological motion task activity, BD = biological motion task dynamics, SA = scrambled motion task activity, SD = scrambled motion task dynamics, LSTM = our method (blue), ROI = individual ROI analysis (red), PCA = principal component analysis (yellow), ICA = independent component analysis (purple). Cyan markers denote statistically significantly different results compared to our LSTM method (paired two-tailed t-test, p < 0.05).

relation of functional network activity for subjects in the test set with the design signals are generally stronger or similar using our LSTM method compared to other approaches (subfigures (a) and (b)). The correlation between the values computed from the training set and the test set are clearly stronger using our LSTM method, particularly for design signals for dynamic changes in biological and scrambled motion tasks (subfigures (c)). Together this suggests that our approach estimates functional networks whose activity patterns (defined by the correlation vectors  $c_{BA}$ ,  $c_{BD}$ ,  $c_{SA}$ ,  $c_{SD}$ ) are more closely replicated across subjects within the same dataset compared to the other methods. Finally, when using functional networks defined by one dataset to estimate functional network activity in the other dataset, we again saw that our approach overall resulted in the larger correlations with the task design signals (subfigures (d) and (e)). This demonstrates that our LSTM approach is able to find more reliable networks that are highly associated with task dynamics across different datasets.

## 4. CONCLUSIONS

We have presented a method for determining more reproducible functional networks whose activity is more strongly associated with a given task paradigm. Our approach uses un-

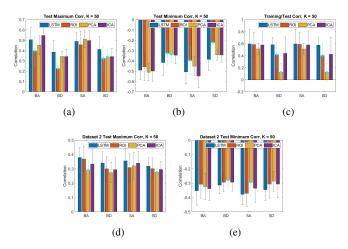


Fig. 2: Results for Dataset 1, with K=50 networks. See Fig. 1 caption for legend.

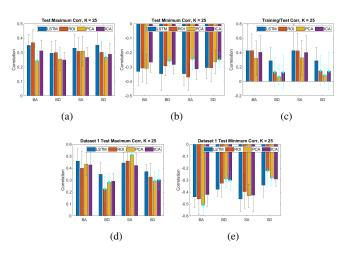


Fig. 3: Results for Dataset 2, with K=25 networks. See Fig. 1 caption for legend.

supervised training of LSTMs to learn to generate the fMRI ROI time-series. We demonstrated stronger correlations between the activity of the LSTM-derived functional networks with the design signals for a biological motion perception task. These results translated better across subjects within the same dataset and across datasets. This suggests the networks found are more reproducible and more reliably characterize the network activity in the brain, which is essential for better characterizing the neural correlates of a target task.

## 5. REFERENCES

 Martin M. Monti, "Statistical analysis of fmri time-series: a critical review of the glm approach," Front. Hum. Neurosci., 2011.

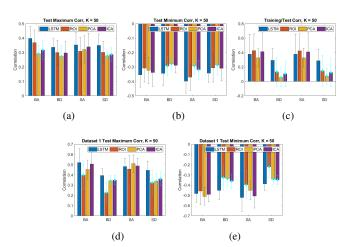


Fig. 4: Results for Dataset 2, with K=50 networks. See Fig. 1 caption for legend.

- [2] S. Hochreiter and J. Schmidhuber, "Long short-term memory," Neural Computation, 1997.
- [3] Umut Güçlü and Marcel A. J. van Gerven, "Modeling the dynamics of human brain activity with recurrent neural networks," *Front Comput Neurosci*, 2017.
- [4] N. C. Dvornek, Xiaoxiao Li, Juntang Zhuang, and J. S. Duncan, "Jointly discriminative and generative recurrent neural networks for learning from fmri," in *MLMI* 2019, 2019, LNCS 11861.
- [5] Ilya Sutskever, Oriol Vinyals, and Quoc V. Le., "Sequence to sequence learning with neural networks," *Advances in neural information processing systems (NIPS 2014)*, 2014.
- [6] M. Kaiser, C. Hudac, S. Shultz, S. Lee, C. Cheung, A. Berken, ..., and K. Pelphrey, "Neural signatures of autism," *Proc Natl Acad Sci U S A*, 2010.
- [7] M. Jenkinson, C. F. Beckmann, T. E. Behrens, M. W. Woolrich, and S. M. Smith, "Fsl," *NeuroImage*, vol. 62, pp. 782–790, 2012.
- [8] Raimon H.R. Pruim, Maarten Mennes, Daan van Rooij, Alberto Ller, Jan K. Buitelaar, and Christian F. Beckmann, "Icaaroma: A robust ica-based strategy for removing motion artifacts from fmri data," *NeuroImage*, 2015.
- [9] N. Tzourio-Mazoyera, B. Landeau, D. Papathanassiou, F. Crivello, O. Etard, N. Delcroix, B. Mazoyer, and M. Joliot, "Automated anatomical labeling of activations in spm using a macroscopic anatomical parcellation of the mni mri single-subject brain," *NeuroImage*, 2002.
- [10] Sashank J. Reddi, Satyen Kale, and Sanjiv Kumar, "On the convergence of adam and beyond," *ICLR*, 2018.
- [11] Vince D. Calhoun, Jingyu Liu, and Tülay Adali, "A review of group ica for fmri data and ica for joint inference of imaging, genetic, and erp data," *NeuroImage*, 2009.
- [12] Hugo Gävert, Jarmo Hurri, Jaakko Särelä, and Aapo Hyvärinen, "FastICA," https://research.ics.aalto.fi/ica/fastica/, 1996-2005.